ELSEVIER

Catalysis Today 49 (1999) 49–56

CATALYSIS TODAY

Hydrogenation of *p*-isobutyl acetophenone using a Ru/Al_2O_3 catalyst: reaction kinetics and modelling of a semi-batch slurry reactor

S.P. Mathew, M.V. Rajasekharam, R.V. Chaudhari*

Chemical Engineering Division, National Chemical Laboratory, Pune 411008, India

Abstract

The kinetics of hydrogenation of *p*-isobutyl acetophenone using a 2% Ru/Al_2O_3 catalyst was studied experimentally in a semi-batch slurry reactor over a temperature range of 373–398 K. The effect of catalyst loading, H_2 partial pressure and *p*-isobutyl acetophenone concentration on concentration–time and H_2 consumption profiles was studied. A rate equation has been proposed based on a Langmuir–Hinshelwood type mechanism in which reaction steps between adsorbed hydrogen and adsorbed liquid phase reactants are assumed to be rate determining. The kinetic parameters were evaluated by fitting the integral batch reactor data at different temperatures. The activation energies, heat of adsorption and the entropy of adsorption of hydrogen and various liquid phase components were evaluated.

Keywords: Hydrogenation; Kinetic modelling

1. Introduction

Hydrogenation of *p*-isobutyl acetophenone (*p*-IBAP) is an important step in a new catalytic route developed for ibuprofen, a non-steroidal, anti-inflammatory drug. This new catalytic route [1] is considered as a major innovation in ibuprofen technology both from environmental as well as economic point of view, as it eliminates the conventional stoichiometric synthetic routes which produce a large amount of salts as by-products. Moreover, this reaction is an excellent example of a complex multistep catalytic hydrogenation leading to a variety of products. Most of the earlier literature on this reaction is patented and there are only a few reports which deal with the catalytic reaction mechanism, kinetic modelling and reaction engineering aspects.

The previous work on hydrogenation of *p*-IBAP is summarised in Table 1. The reduction of a carbonyl group is known to be catalysed by a variety of supported metal catalysts such as Pd, Ni and Ru. During this reaction, reduction of a carbonyl group as well as the benzene ring can occur leading to a variety of products, and hence understanding of the selectivity behaviour is also important. Most of the previous work has reported investigations on the activity and selectivity of the catalysts and some aspects of reaction mechanism using Ni and Pd catalysts. No detailed investigations have been published using Ru catalysed hydrogenation of *p*-IBAP. In this paper, we report the results on kinetic modelling of hydrogenation of *p*-IBAP using 2% Ru/Al_2O_3 as a catalyst. The effect of catalyst loading, partial pressure of hydrogen and initial substrate concentration on the rate of hydrogen consumption as well as the concentration–time behaviour in a semi-batch reactor has

*Corresponding author.

0920-5861/99/$ – see front matter
PII: S0920-5861(98)00407-6

Table 1
Literature on hydrogenation of *p*-isobutyl acetophenone

S. no.	Catalyst	Co-catalyst	Solvent	Reaction condition			Conversion (%)	Selectivity (%)	Reference
				T (K)	Pressure (atm)	Reaction time (h)			
1	Pd/C	–	MeOH	303	6.8	1	99	97	[1]
2	Activated Ni sponge	–	–	333	17.00	1.5	99	–	[2]
3	$Pd/CaCO_3$	–	MeOH	333	8.16	18	85	100	[3]
4	Pd/C	Triethyl amine	MeOH	333	8.16	1	97	100	[4]
5	Pd/C	Aq. NaOH	*n*-Hexane	373	10.50	1.5	99	97	[1]
6	Raney Ni	Pyridine	MeOH	413	68.03	4	87	–	[5]
7	10% Ni/HY	–	MeOH	373	30.00	2	75	75	[6]
8	Ru/C	Aq. NaOH	–	403	4.0	5	97	–	[7]

been studied. Based on these data rate equations have been proposed, following the model discrimination procedure and rate parameters evaluated. Analysis of the rate data for the significance of gas–liquid, liquid–solid and intraparticle diffusion effects has also been discussed.

2. Experimental

The catalyst, 2% Ru/Al_2O_3, was prepared in our own laboratory by the precipitation technique, with following specifications: catalyst particle size: 1×10^{-5} m; particle density: 2×10^{3} kg/m^3; porosity: 0.5; tortousity: 4; Ru content: 2% (w/w).

All the hydrogenation experiments were carried out in a 3×10^{-4} m^3 capacity stirred autoclave reactor made of SS 316 and supplied by Parr Instrument, USA, with provision for operation up to 523 K and 10 MPa pressure. It was equipped with facilities such as automatic temperature control, gas inlet/outlet, sampling of the liquid contents, variable agitation speed, safety rupture disc and pressure transducer. A storage reservoir for H_2 gas was used along with a constant pressure regulator to determine H_2 consumption as a function of time, while maintaining the reactor at a constant desired pressure.

In a typical experiment, *p*-IBAP was charged into the reactor along with the catalyst and solvent, methanol, to make up a total volume of 1×10^{-4} m^3. The reactor was flushed with N_2 and then with H_2 2–3 times at room temperature. The contents were heated to a desired temperature and then pressurised with H_2. Switching the stirrer on started the reaction. Liquid sample was withdrawn at this point and considered as an initial sample. The hydrogen consumption was determined from the pressure drop in the H_2 reservoir vessel as a function of time. Liquid samples were withdrawn at regular intervals of time and analysed by gas chromatographic technique using a HP-6890 Gas chromatograph fitted with a HP-FFAP capillary column (30 m×0.53 μm×0.1 mm film thickness on polyethylene glycol stationary phase). The conditions of GC analysis were as follows: FID temperature: 573 K, column temperature: 438–463 K (programmed at 25 K/min), injection temperature: 523 K, carrier gas: N_2. A few samples were analysed by GC–MS (Shimadzu QP 2000A). The range of operating conditions used in this work are given in Table 2.

3. Results and discussion

3.1. Experimental results

The main objective of this work is to study: (a) intrinsic kinetics of hydrogenation of *p*-IBAP using a

Table 2
Range of parameters

Catalyst loading (kg/m^3)	2.5–10
Agitation speed (Hz)	7.5–15
H_2 partial pressure (MPa)	3.4–6.2
p-IBAP concentration (kmol/m^3)	0.25–1.1
Temperature (K)	373–398
Volume of liquid (m^3)	10^{-4}

2% Ru/Al_2O_3 catalyst in a slurry reactor and (b) performance of a semi-batch slurry reactor under isothermal conditions. For this purpose, a few experiments were first carried out to confirm the product distribution and define a reaction scheme. Catalyst recycle experiments were also carried out without exposing the catalyst to atmosphere and it was found that the activity remains constant during the course of a batch experiment.

A typical concentration–time profile of various components involved in the hydrogenation of *p*-IBAP using 2% Ru/Al_2O_3 is shown in Fig. 2. It was observed that in the initial stages, *p*-IBAP undergoes hydrogenation through two different path ways: (i) hydrogenation of a carbonyl group to give *p*-isobutyl phenyl 2-ethanol (*p*-IBPE) and (ii) ring hydrogenation of *p*-IBAP to 4-isobutyl cyclohexyl methyl ketone (4-IBCMK). The formation of *p*-IBPE was much higher compared to the ring hydrogenated product 4-IBCMK. During the course of reaction *p*-IBPE also undergoes ring hydrogenation to give 4-isobutyl cyclohexyl 2-ethanol (4-IBCHE) where as the formation of 4-IBCHE by ketonic hydrogenation of 4-IBCMK is comparatively very slow. *p*-IBPE undergoes dehydration to form *p*-isobutyl styrene (*p*-IBSTY) which on further hydrogenation gives *p*-isobutyl ethyl benzene (*p*-IBEB). In the range of conditions studied, the formation of *p*-IBSTY was very negligible and hence is not included in the reaction scheme. Ring hydrogenated product of *p*-IBEB, 4-isobutyl ethyl cyclohexane (4-IBECH) was found to be less than 3%. Based on the products identified and characterised by GC and GC–MS, the reaction scheme is shown in Fig. 1.

3.2. Analysis of initial rate

The initial rate of reaction was calculated from substrate and hydrogen consumption data under different conditions. It was important to ensure that the rate data obtained for kinetic analysis were obtained under conditions of chemical reaction control and mass transfer limitations were not significant. In order to calculate the contribution of these mass transfer steps, quantitative criteria suggested by Ramachandran and Chaudhari [8] were used. The observed rate data were compared with maximum rates of gas–liquid, liquid–solid and intraparticle mass transfer rates. The factors α_1, α_2 and ϕ_{exp} were calculated (see Appendix A), which are defined as the ratio of observed rate of reaction to the maximum rates of gas–liquid, liquid–solid and intraparticle mass transfer rates, respectively. This analysis showed that the values of α_1, α_2 and ϕ_{exp} at all temperatures were below 0.05, 0.0003 and 0.08, respectively, showing that these mass transfer effects are negligible. For particle size $dp > 5 \times 10^{-4}$ m, intraparticle diffusion effects were found to be significant. The initial rates

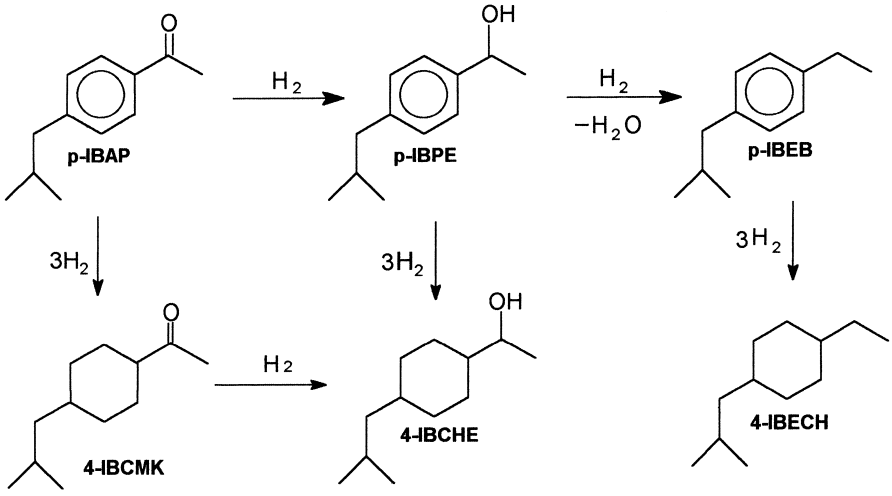

Fig. 1. Reaction scheme for hydrogenation of *p*-IBAP using 2% Ru/Al_2O_3 catalyst.

were found to be independent of stirring speed beyond 600 rpm. Also, the initial rates at different catalyst loading showed a linear dependence. This further supports our conclusion that the gas–liquid mass transfer resistance is not significant.

The general trends observed for the variation of initial rates with different parameters were: (i) the rate of reaction was linearly dependent on H_2 pressure in low pressure range and tending towards zero order at higher pressures, (ii) the rate vs *p*-IBAP concentration passed through a maxima indicating substrate inhibition beyond 0.7 kmol/m^3 concentration. These data, however, represent only the reactions in the initial stages and hence are not useful to develop kinetic models. For this purpose integral concentration–time profiles under different initial conditions should be considered.

3.3. Kinetic modelling

The experimental concentration–time data in the kinetic regime were used to evaluate the different rate equations. Since the formation of *p*-IBECH was negligible in most of the experiments, the reaction scheme shown in Fig. 1 was simplified as shown in Fig. 3. In this scheme, it was assumed that 4-IBCHE is essentially formed from *p*-IBPE hydrogenation and the rate of hydrogenation of 4-IBCMK is negligible. This is consistent with our observation that (see Fig. 2) after *p*-IBPE concentration depletes significantly no further increase in 4-IBCHE formation was observed even though the concentration of 4-IBCMK was significant. In order to develop the rate equations, several assumptions were made: (i) The rate of surface reaction is rate limiting and rate of adsorption and desorption is very high compared to the reaction rate. (ii) Only the reactive species are adsorbed on active sites and sites occupied by solvent are negligible. (iii) The adsorption of saturated product, *p*-IBCHE, was assumed to be negligible due to weak adsorption characteristics [9]. The adsorption of *p*-IBEB was not taken into account, due to its lower concentration and was observed only in the final stages of the reaction, but the adsorption of *p*-IBCMK was taken into account.

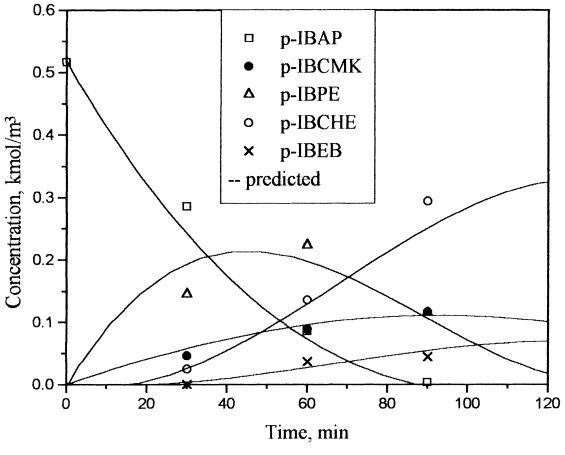

Fig. 2. Concentration–time profile at 398 K. Reaction conditions: concentration of *p*-IBAP: 0.53 kmol/m^3, catalyst loading: 5 kg/m^3, P_{H_2}: 4.67 MPa, solvent: MeOH, agitation speed: 15 Hz.

The following reaction mechanisms were considered to derive rate equations:

1. reaction between associatively adsorbed hydrogen and adsorbed liquid phase components on two different type of sites,
2. reaction between adsorbed hydrogen (associatively) and adsorbed liquid phase components on the same site and
3. reaction between dissociatively adsorbed hydrogen and adsorbed liquid phase components on the same site.

In order to test the applicability of these equations (see Table 3) a semi-batch reactor model was used under isothermal conditions. The material balances of different components are given below for model 2 as an example:

$$\frac{dC_1}{dt} = -(r_1 + r_2) = -\frac{wK_H C_H^* K_1 (k_1 C_1 + k_2 C_1)}{\left(1 + K_H C_H^* + \sum_{j=1,3} K_j C_j\right)^2}, \quad (1)$$

$$\frac{dC_2}{dt} = r_1 = \frac{wk_1 K_H K_1 C_H^* C_1}{\left(1 + K_H C_H^* + \sum_{j=1,3} K_j C_j\right)^2}, \quad (2)$$

$$\frac{dC_3}{dt} = r_2 - r_3 - r_4 = \frac{wK_H C_H^* (k_2 K_1 C_1 - k_3 K_3 C_3 - k_4 K_3 C_3)}{\left(1 + K_H C_H^* + \sum_{j=1,3} K_j C_j\right)^2}, \quad (3)$$

$$\frac{dC_4}{dt} = r_3 = \frac{wk_3 K_H C_H^* K_3 C_3}{\left(1 + K_H C_H^* + \sum_{j=1,3} K_j C_j\right)^2}, \quad (4)$$

Table 3
Comparison of various models for hydrogenation of *p*-isobutyl acetophenone

S. no.	Model	Temp. (K)	Rate constant×100				Adsorption constants				$\phi_{min}\times10^4$
			k_1	k_2	k_3	k_4	K_H	K_2	K_3	K_4	
1	$r_i = \frac{k_i K_H K_j C_j C_H^*}{(1+K_H C_H^*)\left(1+\sum_{j=1,3} K_j C_j\right)}$	373	0.0128	0.0342	0.1211	0.157	0.2739	8.7646	0.3311	2.9057	2.37
		386	0.0213	0.0231	0.0189	0.0361	1.9079	8.9866	−7.5938	2.0907	0.13
		398	0.0058	0.0166	0.0304	0.0784	0.6552	7.6712	−19.560	4.3798	0.21
2	$r_i = \frac{k_i K_H K_j C_j C_H^*}{\left(1+K_H C_H^*+\sum_{j=1,3} K_j C_j\right)^2}$	373	0.5000	0.8588	1.8224	0.141	0.0281	4.5312	0.2137	2.5493	0.11
		386	1.0470	1.3525	3.0736	0.203	0.0226	4.2890	0.1720	2.3524	0.23
		398	1.5192	2.0219	4.4193	0.272	0.0201	4.1263	0.1260	2.1335	0.14
3	$r_i = \frac{k_i (K_H)^{1/2} K_j C_j (C_H^*)^{1/2}}{\left(1+(K_H C_H^*)^{1/2}+\sum_{j=1,3} K_j C_j\right)^2}$	373	0.0247	0.0397	0.2576	0.0331	0.242	9.0544	0.5033	1.2717	0.22
		386	1.2873	1.3399	2.1422	−0.5478	−0.0133	6.1884	−2.5160	3.0693	2.37
		398	0.0123	0.0384	0.0576	0.0163	0.4260	5.4702	−5.9806	3.5582	0.13

$$\frac{dC_5}{dt} = r_4 = \frac{wk_4 K_H C_H^* K_3 C_3}{\left(1 + K_H C_H^* + \sum_{j=1,3} K_j C_j\right)^2}. \quad (5)$$

The initial conditions are

$$\text{at } t = 0, \quad C_1 = C_{10} \quad \text{and} \quad C_2 = C_3 = C_4 = C_5 = 0. \quad (6)$$

Here k_1, k_2, k_3 and k_4 represent the rate constants of steps r_1, r_2, r_3 and r_4, respectively, in the scheme shown in Fig. 3. K_H, K_1, K_2 and K_3 represent the adsorption constants of various components and C_H^*, C_1, C_2 and C_3 their concentrations, respectively.

The total rate of hydrogenation is given by

$$R_{H_2} = 3r_1 + r_2 + 3r_3 + 2r_4 \quad (7)$$

In order to select a suitable rate equation, a non-linear least square regression analysis was used for each rate equation to obtain the best fit values of the parameters. For this purpose, an optimisation program based on Marquarts method combined with a Runge–Kutta method was used. The solubility of hydrogen

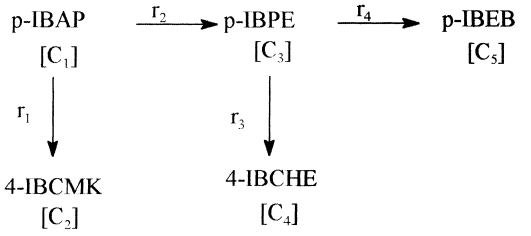

Fig. 3. Simplified reaction scheme.

required for calculation of $C_H^*(P_{H_2} \times H_e)$ for different *p*-IBAP concentrations was determined at different temperatures. These data are presented in Table 4.

The model parameters were estimated by minimising the objective function

$$\phi_{min} = \sum_{i=1}^{5} \sum_{i=1}^{n} \left(Y_{i_{exp}} - Y_{i_{mod}}\right)^2, \quad (8)$$

where $Y_{i_{exp}}$ is the measured concentration of component i, $Y_{i_{mod}}$ is the calculated concentration of component i and n is the number of samples. The rate

Table 4
Solubility of H_2 in *p*-IBAP and MeOH mixtures

Temperature (K)	Henry's constant×10^3 (kmol/m^3/atm)		
	5% *p*-IBAP+95% MeOH	10% *p*-IBAP+90% MeOH	15% *p*-IBAP+85% MeOH
373	4.388	4.748	5.324
386	5.084	6.035	6.073
398	6.631	7.578	7.219

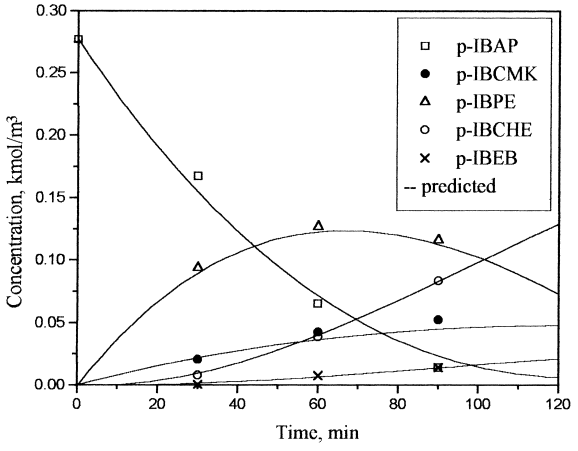

Fig. 4. Concentration–time profile at 373 K. Reaction conditions: concentration of *p*-IBAP: 0.27 kmol/m^3, catalyst loading: 5 kg/m^3, P_{H_2}: 4.76 MPa, solvent: MeOH, agitation speed: 15 Hz.

parameters estimated and ϕ_{min} values are given in Table 3. Out of the three models considered, models 1 and 3 gave negative values for some constants and therefore were rejected. Model 2 was found to be the best to represent the kinetics of hydrogenation of *p*-IBAP using 2% Ru/Al_2O_3 catalyst. The experimental and the predicted concentration–time data were found to agree within 5–8% error as shown in Figs. 4 and 5.

From the temperature dependence of rate parameters (Figs. 6 and 7), the activation energies of various reaction steps were calculated. These values

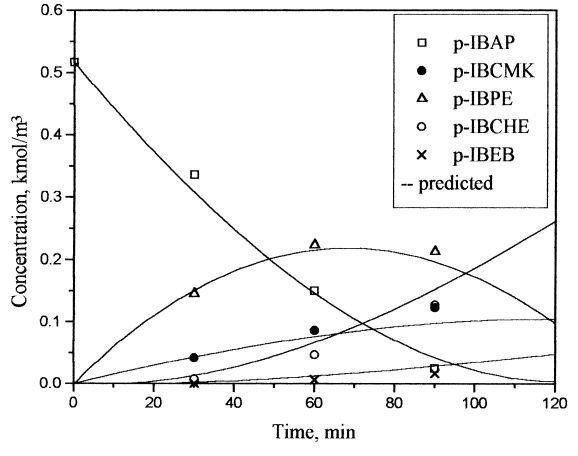

Fig. 5. Concentration–time profile at 386 K. Reaction conditions: concentration of *p*-IBAP: 0.53 kmol/m^3, catalyst loading: 5 kg/m^3, P_{H_2}: 4.76 MPa, solvent: MeOH, agitation speed: 15 Hz.

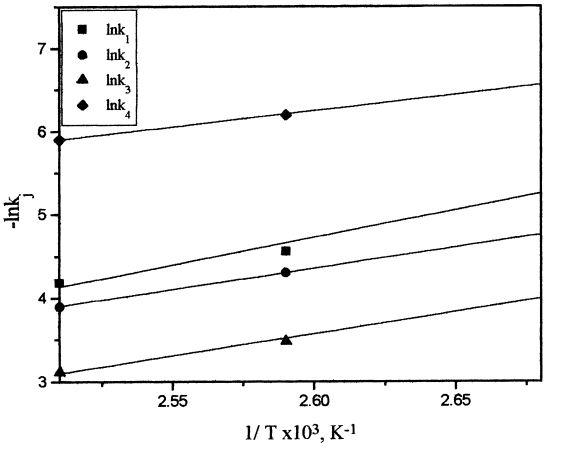

Fig. 6. Temperature dependence of rate constants.

of activation energies for steps r_1, r_2, r_3 and r_4 were found to be 47, 42, 44 and 57 kJ/mol, respectively. The enthalpy of adsorption and the entropy of adsorption of hydrogen and various liquid components were also calculated (see Table 5) as follows [10]:

$$K_i = K_{i_0} \exp\left(-\frac{\Delta H_i}{RT}\right), \tag{9}$$

$$K_{i_0} = \exp\left(\frac{\Delta S_i}{R}\right), \tag{10}$$

K_{i_0}, ΔH and ΔS represent the pre-exponential factor, enthalpy and entropy of adsorption, respectively. The observation of adsorption enthalpy $-\Delta H > 0$ and

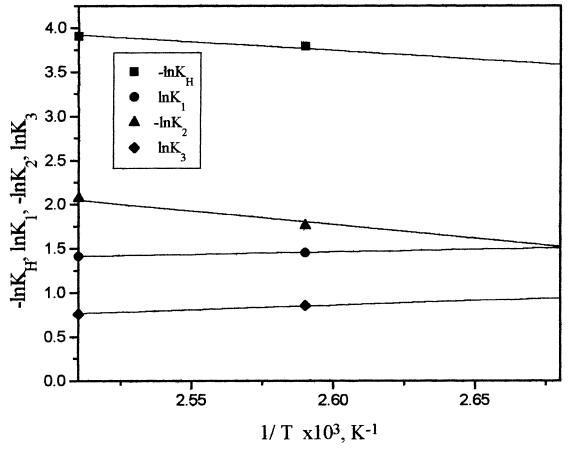

Fig. 7. Temperature dependence of adsorption constants.

Table 5
Values of ΔH and ΔS

Adsorbing species	$-\Delta H$ (kJ/mol)	$-\Delta S$ (J/mol K)
H_2	17	75
p-IBAP	5	5
4-IBCMK	26	83
p-IBPE	9	16

$-\Delta S>0$ also indicate that the rate parameters obey the Arrhenius temperature dependence.

4. Conclusion

Hydrogenation of *p*-IBAP using a 2% Ru/Al_2O_3 catalyst was studied in a slurry reactor for a temperature range of 373–398 K. The products *p*-isobutyl phenyl 2-ethanol, 4-isobutyl cyclohexyl methyl ketone, 4-isobutyl cyclohexyl 2-ethanol, *p*-isobutyl ethyl benzene and 4-isobutyl ethyl cyclohexane were characterised by GC–MS. The effect of catalyst loading, *p*-isobutyl acetophenone concentration and H_2 pressure on concentration–time profile was studied and a detailed kinetic analysis has also been presented. The accuracy of rate model and discrimination of various rate models are discussed. A rate model based on competitive, nondissociative adsorption of hydrogen and different liquid phase components followed by surface reaction found to fit well the concentration–time profile at all temperatures. The rate parameters were determined and activation energies calculated corresponding to each rate constant. Similarly, from the temperature dependence of adsorption constants, heat of adsorption and entropy values were also evaluated.

5. Nomenclature

$C^*_{H_2}$	saturation solubility of H_2 (kmol/m^3)
$C_{1,0}$	concentration of *p*-isobutyl acetophenone at $t=0$ (kmol/m^3)
C_1	concentration of *p*-isobutyl acetophenone (kmol/m^3)
C_2	concentration of 4-isobutyl cyclohexyl methyl ketone (kmol/m^3)
C_3	concentration of *p*-isobutyl phenyl ethanol (kmol/m^3)
C_4	concentration of 4-isobutyl cyclohexyl ethanol (kmol/m^3)
C_5	concentration of *p*-isobutyl ethyl benzene (kmol/m^3)
d_p	catalyst particle diameter (m)
D_M	molecular diffusivity (m^2/s)
D_e	effective diffusivity (m^2/s)
ΔE	activation energy (kJ/mol)
ΔH	enthalpy of adsorption (kJ/mol)
H_e	Henry's constant (kmol/m^3/atm)
k_1, k_2, k_3, k_4	reaction rate constants (m^3/kg) (m^3/kmol s)
K_1, K_2, K_3	adsorption equilibrium constants (m^3/kmol)
K_H	adsorption equilibrium constant for hydrogen (m^3/kmol)
$k_L a_b$	gas–liquid mass transfer coefficient (s^{-1})
k_s	liquid–solid mass transfer coefficient (m/s)
N	speed of agitation (Hz)
P_{H_2}	partial pressure (atm)
r_1–r_4	reaction rates of respective steps in Fig. 3 (kmol/m^3/s)
R_{H_2}	total rate of hydrogenation (kmol/m^3/s)
ΔS	entropy change (J/mol K)
U_g	gas velocity (m/s)
V_L	liquid volume (m^3)
w	catalyst weight (kg/m^3)

Greek letters

α_1	parameter defined in Appendix A
α_2	parameter defined in Appendix A
ϕ_{exp}	parameter defined in Appendix A
ϕ_{min}	parameter defined in Eq. (8)
μ_l	viscosity of liquid (P)
ϵ_p	porosity of the catalyst particle
ρ_p	particle density (kg/m^3)
ρ_g	density of gas (kg/m^3)
ρ_L	density of liquid (kg/m^3)
τ	tortousity factor

Acknowledgements

We would like to thank Dr. R. Jaganathan for his valuable discussions during this work. One of the authors S.P. Mathew would like to thank CSIR for providing him a research fellowship.

Appendix A

For ascertaining the contribution of various mass transfer resistances, the following criteria described by Ramachandran and Chaudhari [8] were used:

1. Absence of gas–liquid mass transfer can be considered unimportant if

$$\alpha_1 = \frac{R_{H_2}}{k_l a_b C^*_{H_2}} < 0.1. \quad (A.1)$$

2. The liquid–solid mass transfer resistance can be considered to be negligible if

$$\alpha_2 = \frac{R_{H_2}}{k_s a_p C^*_{H_2}} < 0.1, \quad (A.2)$$

where

$$a_p = \frac{6w}{\rho_p d_p}. \quad (A.3)$$

3. Pore diffusion is considered to negligible if

$$\phi_{exp} = \frac{d_p}{6}\left[\frac{(m+1)}{2D_e}\frac{\rho_p R_{H_2}}{wC^*_{H_2}}\right]^{1/2} < 0.2, \quad (A.4)$$

where D_e represents the effective diffusivity which is given as

$$D_e = D_M \epsilon/\tau. \quad (A.5)$$

The molecular diffusivity, D_M, is evaluated from the following correlation proposed by Wilke and Chang [11].

The gas–liquid mass transfer, $k_L a_b$, was evaluated from the correlation proposed by Bern et al. [12] for a stirred tank reactor

$$k_l a_b = 1.099 \times 10^{-2} N^{1.16} d_I^{1.797} u_g^{0.32} V_L^{-0.52} \quad (A.6)$$

For calculation of k_s, the correlation proposed by Sano et al. [13] was used:

$$\frac{k_s d_p}{DF_c} = 2 + 0.4\left[\frac{e d_p^4 \rho_L^3}{\mu_L^3}\right]^{0.25}\left[\frac{\mu_L}{\rho_L D_M}\right]^{0.333} \quad (A.7)$$

where F_c is the shape factor assumed to be unity for spherical particle and e, the energy supplied to the liquid, was calculated by the procedure described by Calderbank [14].

References

[1] V. Elango, Method for producing ibuprofen, Eur Patent 400 892 (Cl.C07c57/30), CA:114:206780, to Hoest Celanese and Boots, 1990.

[2] D.A. Ryan, Method for producing 1-(4-isobutyl phenyl) ethanol, Eur. Patent 358 420 (Cl.c07c33/20), CA:113:77897, to Hoest Celanese and Boots, 1990.

[3] K. Saeki, U. Takashi, Preparation of aromatic carbinols, Jpn. Kokai Tokkyo Koho JP. 0 273 027, CA:113:58673, to Daicel Chemical Ind. Ltd., 1990.

[4] K. Saeki, K. Shima, Preparation of aromatic carbinols from aromatic ketones, Jpn. Kokai Tokkyo Koho JP. 0 262 837 (Cl.C07C33/20), CA:113:58672, to Daicel Chemical Ind. Ltd., 1990.

[5] H. Yoshiyaki, Hydrogenation of aromatic ketones with Raney Ni-amine catalyst, Jpn. Jpn. Kokai Tokkyo Koho JP. 63 630 432 (Cl.C07C33/20), CA:110:7852, to Daicel Chemical Ind. Ltd., 1988.

[6] M.V. Rajashekharam, Thesis, University of Pune, India, 1997.

[7] T. Tadashi, Y. Yukituro, Y. Sangi, A process for preparation of 1-(1-hydroxy ethyl) alkyl cyclohexanes by catalytic hydrogenation of alkyl acetophenones, Jpn. Kokai Tokkyo Koho JP. 62 185 032, 108:167018, to Takiho Pharmaceutical Company, 1987.

[8] P.A. Ramachandran, R.V. Chaudhari, Three Phase Catalytic Reactors, Gordon and Breach, New York, 1983.

[9] G. Neri, L. Bonaccorsi, Kinetic analysis of cinnamaldehyde hydrogenation over alumina-supported ruthenium catalysts, Ind. Eng. Chem. Res. 36 (1997) 3554.

[10] X.D. Zhu, G. Valerius, H. Hofmann, Th. Haas, D. Arntz, Intrinsic kinetics of 3-hydroxypropanal hydrogenation over $Ni/SiO_2/Al_2O_3$ catalyst, Ind. Eng. Chem. Res. 36 (1997) 2897.

[11] C.R. Wilke, P. Chang, Correlation of diffusion co-efficients in dilute solutions, AIChE J. 1 (1955) 264.

[12] L. Bern, M. Hell, N.H. Schoon, Kinetics of hydrogenation of rapeseed oil. Rate equations of chemical reactions, J. Am. Oil. Chem. Soc. 52 (1975) 391.

[13] Y. Sano, N. Yamaguchi, T. Adachi, Mass transfer coefficients for suspended particles in agitated vessels and bubble columns, J. Chem. Eng. Jpn. 1 (1974) 255.

[14] P.H. Calderbank, Physical rate processes in industrial fermentation Part I. The interfacial area in gas–liquid contacting with mechanical agitation, Trans. Inst. Chem. Eng. 36 (1958) 443.